J Mater Sci (2012) 47:4236–4250
DOI 10.1007/s10853-011-6081-8

Carbon fibres from cellulosic precursors: a review

Ahu Gümrah Dumanlı · Alan H. Windle

Received: 3 August 2011 / Accepted: 22 October 2011 / Published online: 23 February 2012

Abstract The focus of this review is primarily on the sequence of structural changes at micro and molecular level during carbonization of cellulosic fibres. The influence of various operational parameters such as the pyrolytic temperature and the stabilization agents also discussed as is the effect of the initial properties of the cellulose fibre on the final properties of the carbon fibre.

Abbreviations

AC	Alternative current
ACF	Activated carbon fibre
BC	Bacterial cellulose
^{13}C NMR	Carbon-13 nuclear magnetic resonance spectroscopy
CF	Carbon fibre
CNT	Carbon nanotube
CP/MAS	Cross polarized magic angle spinning
CSA	Chemical shift anisotropy
DC	Direct current
DP	Degree of polymerization
FTIR	Fourier transform infra-red spectroscopy
HTT	Heat treatment temperature
MWNT	Multi wall carbon nanotube
N/tex	Tensile strength unit expressed in force divided by linear density which is numerically equivalent to Gpa/specific gravity
NMMO	*N*-methylmorpholine-*N*-oxide
PAN	Polyacrylonitrile
SEM	Scanning electron microscope
STM	Scanning tunneling microscopy
SWNT	Single wall carbon nanotube
tex	Linear density unit which is equal to the grams per kilometre of material
TGA	Thermal gravimetric analysis
XRD	X-ray diffraction

A. G. Dumanlı · A. H. Windle (✉)
Department of Materials Science and Metallurgy, University of Cambridge, New Museums Site, Pembroke Street, Cambridge CB2 3QZ, UK
e-mail: agd33@cam.ac.uk

Introduction

The exceptional mechanical properties and low density of carbon fibre make it an attractive material for a number of advanced and high-volume applications. The most practical method of producing carbon fibres is carbonization of organic fibres with, today, the majority of carbon fibres being produced from a polyacrylonitrile (PAN) precursor because of their good mechanical properties and high yield. Other viable precursors are cellulosic fibres and mesophase pitch.

Cellulosic precursor fibre was first used by Thomas Edison in the 1880s as the basis for his revolutionary electric lamp filament [1]. Much later, in 1959, the National Carbon Company introduced a carbon cloth from a rayon precursor in 1959 and 2 years later carbon yarn was became available [2, 3]. In 1965, the Thornel range of carbon fibres was announced where properties were improved by a post-carbonization treatment involving stretching at 2500 °C. This fibre had a tensile strength of 1.25 GPa and a Young's modulus of 170 GPa [4]. However, due to the cost of the hot stretching process and the disadvantage of the yield and mechanical properties of the cellulose precursor [5] the production of these fibres had stopped lasted little more than 10 years [6]. Since then carbon fibres based on PAN have been the market leader.

However, these fibres are less suitable for heat shielding and ablative applications due to their high alkaline metal content introduced as a result of the chemical stabilization treatment stages using hydrogen peroxide in an alkaline medium [7]. PAN is also an expensive precursor to start with (9.3 $/kg contribution from PAN precursor towards a total production cost of 17 $/kg carbon fibre) [8, 9]. Furthermore the cost of petroleum-based PAN changes continuously with the fluctuations of the crude oil prices, which cause the carbon-fibre production, costs to vary constantly. In addition, in order to produce sufficient carbon fibre for the worldwide car industry, i.e. 10–100 kg for each car and 50 million cars (on average), the current worldwide carbon-fibre production will require an increase of 5–50-fold. Possibly because of these factors, there has been a recent resurgence of interest in renewable cellulosic precursors as illustrated by Fig. 1. In particular, the cellulosic route is encouraged not only by the low precursor cost, but also by the high thermal conductivity, purity and mechanical flexibility of the resultant fibres[10]. At present, carbon fibre based on cellulose amounts only 1–2% of the total carbon-fibre production [11]. The main producers of cellulose-based carbon fibres are RUE-SPA-Khimvolokno (Republican Unitary Enterprise Svetlogorsk Production Association, Belarus) and SGL Carbon, in Germany.

This review sets recent progress in the science and technology of carbon fibre based on cellulosic precursors in the full historical context, and considers the future prospects for this production route.

Carbon fibres, precursors, structure and properties

Polymeric materials, which yield a carbon residue while not melting during the pyrolysis process are considered to be potential precursors for carbon-fibre production [12]. A good carbon-fibre precursor should also have some additional physical characteristics such as a round cross-section, small linear density, high strength and modulus and fewer defects within the structure [13]. The carbon content of the carbon fibre should also be greater than 90% by weight regardless of the precursor material. The basic structure of carbon fibres is well understood consisting of turbostratic layers of graphene oriented so that they contain the fibre axis (turbostratic layers imply graphene stacked without full crystallographic register, with successive sheets in random rotational settings about their normal sans a resultant spacing of 0.344 nm as opposed to 0.335 nm for the graphite crystal) [7].

The cross-sectional microstructure and the alignment of the graphitic layers along the fibre axis are really crucial for the modulus of the carbon fibre. These two microstructural characteristics of the carbon fibre are mainly formed during the production of the precursor and usually perfected during carbonization. The possible cross-sectional microstructure forms of the carbon fibres are given in, Fig. 2. It has been demonstrated that the transverse texture affects the graphitizability as well; fibres with radial transverse structure are more easily graphitized than fibres with random transverse structure [17]. As shown by Franklin [18–20], there is a distinction between graphitizable and non-graphitizable carbons. Graphitizable carbons show good planar alignment and stacking of graphene layers, on the other hand non-graphitizable carbons do not have long-range parallel order of graphene layers as shown in Fig. 3. In order to achieve high-mechanical performances, especially with respect to axial stiffness, it is necessary to be able to graphitize the precursor. In general,

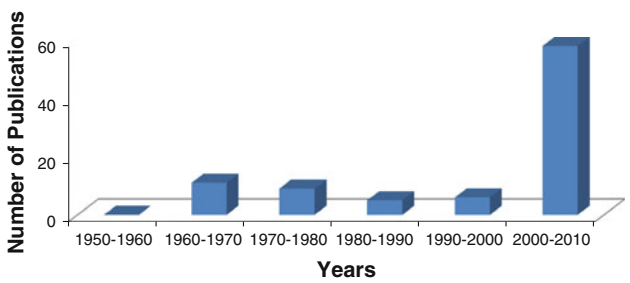

Fig. 1 Number of research publications on carbonization of cellulosic precursors

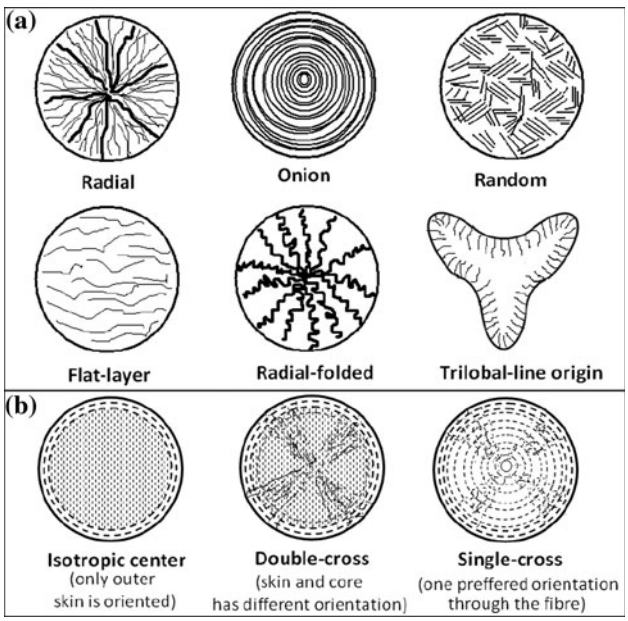

Fig. 2 Schematic representation of cross-sectional micro textures of carbon fibres from different precursors. **a** The pitch-based carbon fibres. **b** PAN-based carbon fibres, redrawn from [14–16]

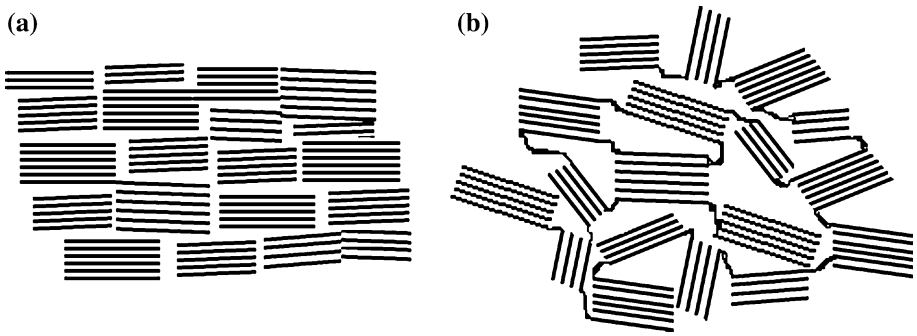

Fig. 3 Illustration of differences between **a** graphitizable carbon and **b** non-graphitizable carbon structures, redrawn from [18]

non-melting solids such as cellulose belong to the non-graphitizable carbon class [21]. However, special types of native cellulose such as tunicate based and bacterial cellulose (BC) have very high crystallinity compared to the common sources of cellulosic carbon which are those of higher plants, may extend the capability for graphitization.

Polyacrylonitrile (PAN) is the most commonly used carbon-fibre precursor today, the process having been developed to yield optimum mechanical properties. The theoretical carbon yield of PAN precursors is 67%. The PAN itself contains polar nitrile groups which hinders the alignment of the molecular chains during spinning. Therefore, a copolymer of PAN and other monomers such as acrylic acid, methacrylic acid and methacrylate in the range of 2–15% is used for carbon-fibre production. Producing carbon fibres from PAN involves thermal stabilization (heat treatment in air between 200 and 300 °C), carbonization (heat treatment under inert atmosphere between 1000 and 1700 °C) and graphitization (heat treatment between 2500 and 3000 °C) [22].

Another common precursor for carbon-fibre production is pitch; both isotropic and mesophase pitches are used to produce carbon fibres. In a mesophase pitch, the planar aromatic molecules, assume a preferred orientation in the liquid phase, tending to lie parallel to each other, a liquid mesophase structure referred to as discotic nematic. Petroleum or coal-tar-based pitch is made up of fused aromatic rings and the theoretical yield is around 80% for the carbon-fibre production. The carbon fibres from these sources are, in principle, capable of having a high modulus almost equal to that of graphite single crystal ($\sim$1050 GPa), which is significantly higher than the high-modulus PAN-based carbon fibres [23]. Furthermore, pitch-based carbon fibres have demonstrated better electrical and thermal properties than PAN-based fibres [22]. However, there are many variations in the pitch structure such as internal voids and surface defects and other contaminations that cause reduction in the mechanical properties [24].

Overall, considerable progress has been made in the last 40 years for understanding the fundamental material-process interactions to be able to produce high-performance carbon fibres from PAN and pitch precursors. However, the challenges regarding these precursors such as, the development of alkaline-free PAN and production of smaller diameter fibres will tend to increase the production costs, which in the very competitive high-performance materials market, are crucial. Melt-spinning has been suggested as a route to produce the alkaline-free PAN fibre [25]. However, commercial PAN copolymer precursors thermally decompose below their melting temperature, making melt-spinning difficult if not impossible. This issue can be resolved by introduction of melt-spinnable PAN copolymers. Although the melt-spinnable copolymer might appear to be attractive as a carbon-fibre precursor, the carbonization steps are changed drastically by the insertion of methyl acrylate co-monomer into the PAN structure [26]. Therefore, the perfection of this system will require more intensive research and development work. Significantly cheaper precursors such as cellulose and lignin, notwithstanding their lower theoretical carbon yield (44.4% for cellulose) are thus the focus of increasing attention, in establishing an enhanced scientific basis on which to decide whether a further development thrust might be worthwhile. Table 1, is a short summary of mechanical properties of carbon-fibres produced using different precursors.

Table 1 Properties of carbon fibres from different precursors

Carbon fibre	Density (g/cm^3)	Tensile strength (GPa)	Tensile modulus (Gpa)	Elongation at break (%)	Diameter (μm)	Ref.
PAN-based CF	1.70–1.80	3.5–6.3	200–500	0.8–2.2	5–10	[27]
Pitch-based CF	1.80–2.20	1.3–3.1	150–900	0.3–0.9	10–11	[28]
Rayon-based CF	1.40–1.50	0.5–1.2	40–100		5–10	[29]
Lyocell-based CF		0.9–1.1	90–100	1.0–1.1	8	[11, 30]

Carbonization of cellulose

Cellulose is a promising precursor for carbon-fibre production; the cellulose fibres have a nicely ordered crystalline structure and cellulose undergoes thermal decomposition without melting. Furthermore, through pyrolysis it forms a strong fibrous carbonaceous material and cellulosic precursors have high thermal conductivity, high purity, mechanical flexibility and low precursor cost. The regenerated cellulose fibre precursors used to make carbon fibres are textile-grade rayon, cuprammonium rayon or viscose rayon [31, 32]. The carbon fibres made from these precursors usually have some defects such as a large void content and interfilament de-bonding, which detract from mechanical properties, leading to weak and brittle carbon fibres, after carbonization [30]. Studies showed that degree of polymerization (DP), aspect ratio of individual nanofibrils within the hierarchical structure of cellulose, Fig. 15 and the orientation of these nanofibrils along the fibre axis are the most important parameters for the production of carbon fibres with good mechanical properties. Yoneshiga and Teranishi [33] reported on the effect of DP of the cellulose on the mechanical properties. They found that using cellulose with a DP higher than 450 instead of conventional rayon (DP about 250), increased the tensile strength of the carbon fibres by approximately 30% after being carbonized at 800 °C [33]. Nevertheless, rayon fibre is still a major raw material for producing activated carbon fibres (ACF) [34], which are produced from carbon fibres through a high-temperature process in an oxidizing atmosphere, (such as carbon dioxide or steam) leading to a high surface area and a highly porous material.

Natural fibres, such as cotton and ramie, have not been favoured for carbonization because of their discontinuous filament structure, and low degree of orientation. They also have impurities arising from the complex structure of natural cellulose sources such as lignin and hemicellulose. However, with development of new processing techniques to make continuous fibres from natural cellulose fibres opens new possibilities to use full advantage of this exceptional structure for advanced applications. The development of the new generation regenerated cellulose (Lyocell) fibres opened new possibilities to use cellulose for carbon-fibre production. Lyocell fibres are spun from cellulose solutions by dissolving cellulose pulp in *N*-methylmorpholine-*N*-oxide (NMMO) as the solvent [35]. The advantage of using this solvent system is that cellulose polymer chains maintain a high degree of polymerization and Lyocell fibres have high crystallinity in which crystalline domains of cellulose-II structure are continuously oriented and dispersed along the fibre axis. These structural properties offer good strength to Lyocell. Furthermore, Lyocell has desirable properties such as its round cross-section, and thermal stability [36]. Therefore, Lyocell fibre is considered to be a promising precursor candidate and a number of publications and patents support Lyocell as a competitive precursor [10, 11, 30, 37, 38], though its use as the basis for industrial carbon-fibre production is not yet established.

The carbonization of cellulose is usually a three step process;

Stabilization

Cellulose is a glucose based, linear polymer connected by β-(1-4) glycosidic linkages, as illustrated in Fig. 4. The hydroxyl groups present in the cellulose structure readily forms intra and inter molecular hydrogen bonds which would give rise to various ordered crystalline arrangements. Based on the molecular stoichiometry $(C_6\ H_{10}O_5)_n$ the theoretical carbon yield of carbonization process of cellulose structure is 44.4%, however, the actual yield is only between 10 and 30%. This is due to depolymerisation of the macromolecular chains, and oxygen taking away carbon as carbon monoxide (CO) and carbon dioxide (CO_2), aldehydes, organic acids and tars [7]. Nevertheless, the pyrolytic mechanism can be modified and stabilized by using proper chemicals such as impregnants or flame retardants to reduce the loss thereby improving the yield and properties of the products and achieving higher efficiency, close to the theoretical limit and therefore lower the cost [39]. Therefore, selection of suitable stabilizer materials is essential for the carbonization process [34, 40].

Degradation of native cellulose fibres starts at 200 °C and ends around 380 °C, under inert atmosphere as shown in the TGA thermogram, Fig. 5. The thermal stability of various cellulose sources depends on the process conditions for cellulose fibre production; the typical rayon precursor starts to degrade at 240 °C [41] and degradation of Lyocell fibre starts at 290 °C [42]. Although the physicochemical processes taking place during the transformation of cellulose into carbon are complex, it is certain that

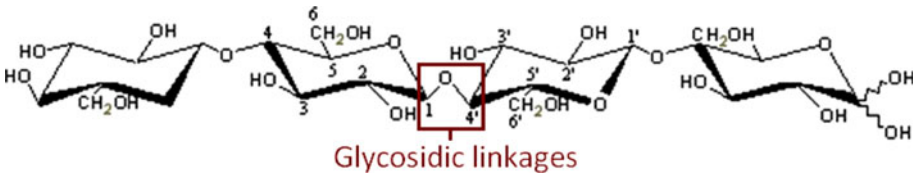

Fig. 4 Cellulose polymer chain

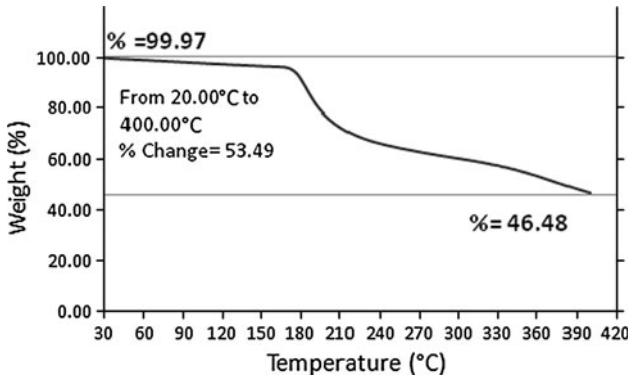

Fig. 5 Typical TGA curve in N_2 for cotton cellulose fibre

depolymerisation of the macromolecular chains produces a variety of oxygenated compounds. This leads to the major mass loss of the solid residue through the production of volatile substances. Two methods can help to reduce the burning loss thereby improving the yield and properties of the carbon fibres from cellulose precursors; pyrolysing cellulose at slow heating rates of a few °C h^{-1} [31, 43] or treatment of cellulose fibre with suitable impregnants [34].

As it is demonstrated in Fig. 6, the pyrolysis of cellulose is controlled mainly by two predominant reactions, dehydration and depolymerization (cleavage). At low temperatures (<300 °C), the favoured reaction is the dehydration reaction which stabilizes the cellulose structure. During the dehydration, elimination of the hydroxyl groups results in double bonds, conjugated double bonds, and subsequently, in an aromatic structure at the carbonization step, one consequence is that the dehydrated cellulose ring becomes less accessible to cleavage through the than the original cellulose structure. The polymeric structure is basically retained through dehydration and at this temperature range weight loss is usually limited to the evaporation of water. Depolymerization at the early stages of pyrolysis without the complete dehydration of the structure leads to small, volatile fragments and causes major mass loss at higher temperatures. Therefore, application of slow heating rates of a few °C h^{-1} can be used to increase the yield of the carbonization. This difference in reaction mechanism of slow pyrolysis is also expected to be reflected in the final fibre properties such as improved density, porosity and microstructure compared to fast pyrolysis products [44].

Another way to improve the yield and properties of the carbon fibres is the treatment of cellulose fibre with suitable impregnants. While studies of carbon fibre conversion from cellulose precursors have been conducted [45–50], there have been relatively few reports on the effect of the impregnants on conversion yield. There are many chemicals that may be used as impregnants for rayon-based activated carbon fibre; the first choice is the Lewis acids, such as zinc and calcium chloride [51, 52], which can also serve as flame retardants for cellulosic materials and have hence been studied widely for many years for that purpose [34]. But strong acidic retardants can easily enhance the formation of levoglucosan (Fig. 6-Stage 3) a carbon-containing bridge-structured volatile substance [53]. Formation of such volatile compounds lowers the carbon yields for manufacturing rayon-based carbon fibre. The change in the pyrolysis mechanism by incorporation of metal ions is not clearly revealed. However, a noteworthy suggestion came from Piskorz et al. [54] that the polar alkaline cations may capture the free ends of the cellulose chains and thereby hinder the "unzipping" reaction which leads to formation of levoglucosan.

Another choice of impregnants is inorganic phosphates and sulphates with nitrogen which have flame retardant effects; however, the efficiency of these impregnants on the carbon-fibre formation and mechanical properties of the final product has not been reported systematically. Phosphate and ammonium salts, particularly dibasic ammonium phosphate $[(NH_4)_2HPO_4]$ and ammonium dihydrogen phosphate $[NH_4H_2PO_4]$ have been used for carbon-fibre production from rayon-based precursors [2, 8]. Nevertheless, it has not been examined in detail how these salts affect the carbonization yield and which parameters are effective on the performance of these types of flame retardants. Zeng et al. [34] worked on a series of phosphate and sulphate salts, and found that all the impregnated materials increase the carbon-fibre formation yield by 50–70% relative to the absence of impregnant. Their work also showed that for the formation of carbon fibre from rayon in the presence of air, $[(NH_4)_2HPO_4]$ is the best impregnant compound giving the highest yield and largest specific surface area. Following this, ammonium dihydrogen phosphate $[NH_4H_2PO_4]$ and phosphoric acid are classified as good impregnants with relatively higher yields as well. Ammonium phosphate is classified as fair, and ammonium sulphate is categorized as a poor impregnant which showed the worst performance among all the compounds.

In addition to flame retardant compounds, use of organosilicon compounds for improving the carbonization yield has previously been patented [55, 56] and studied in the literature as well [57, 58]. The metal oxides are known to improve the thermal stability and oxidation resistance for carbon materials [59]. However, the effects of organosilicon compounds on the carbonization process and the properties of the final carbon fibres have been poorly described and the mechanisms of their action on the pyrolysis processes of converting cellulose into carbon have not been established successfully either. More recent work carried out by Plaisantin et al. [48] using organosilicon compounds showed important differences in the ultimate mechanical properties

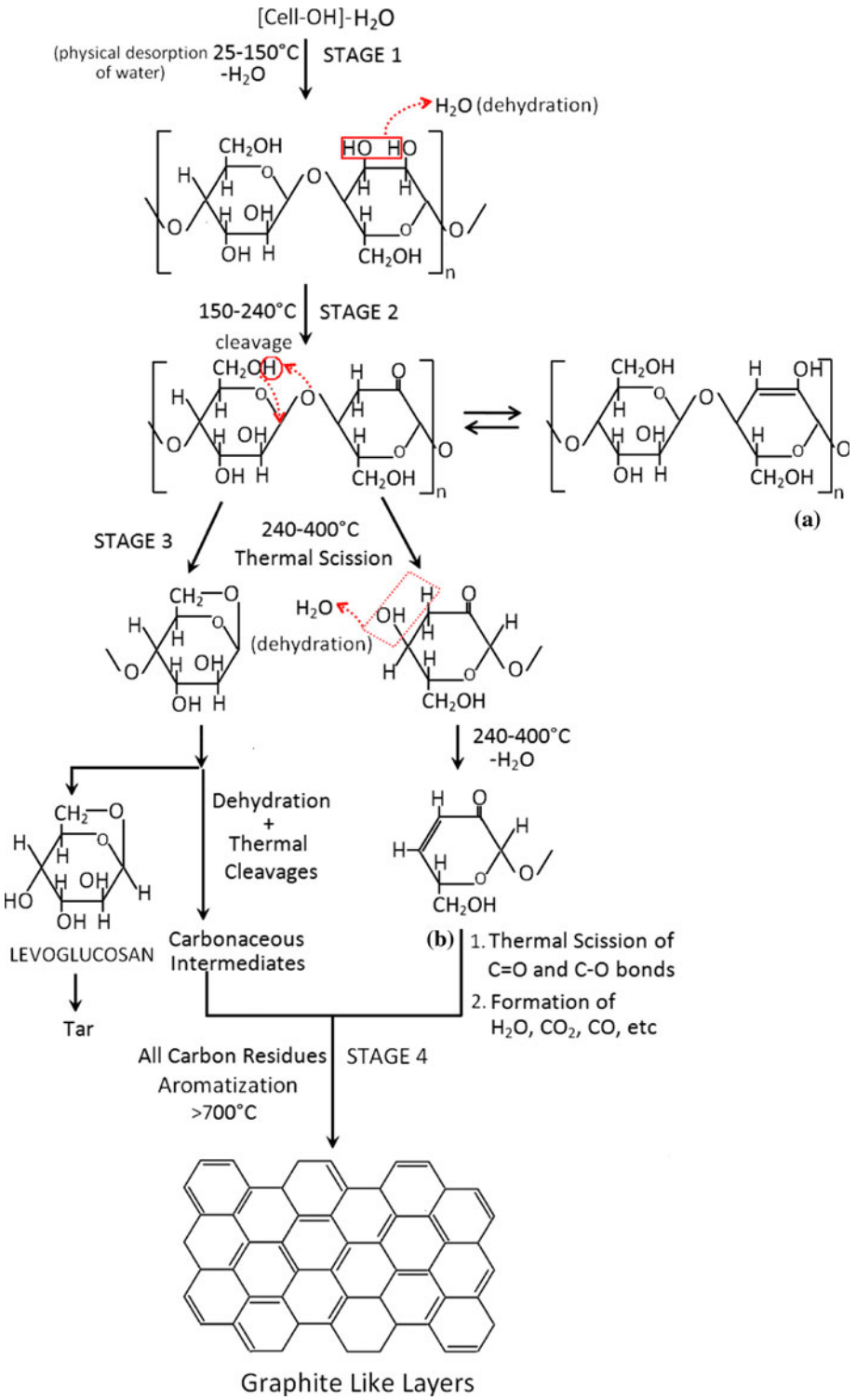

Fig. 6 Reactions involved in conversion of cellulose into carbon fibres, adapted from [41]

of the carbon fibres formed. If the rayon fibres were not treated with an impregnant, the carbonisation led to low tensile strength irrespective of the heating rates, whereas the existence of organosilicon impregnant during carbonization, led to a significant improvement on the tensile strength which was about twice as high as those of fibres obtained via conventional pyrolysis process. Their hypothesis for the role of the additive is based on organosilicon impregnants reducing the size and number of the critical surface defects that cause failure in mechanical properties [48].

Carbonization

As we have seen the first oxidative processes during pyrolysis take place between 25 and 150 °C, while the physical desorption of water and dehydration of the cellulosic unit continues between 150 and 240 °C, which is summarized in Fig. 6 (Stages 1 and 2). This leads to formation of double bonded intermediates, Fig. 6-product-A. Carbonization of cellulose is the process of conversion from this depolymerised structure into graphite-like layers through re-polymerization, i.e. begins at approximately 300 °C and continues to 900 °C, as shown in Fig. 6 (Stages 3 and 4). The basic microstructure of the carbon forms during Stage-3 [47]. As can be seen in Fig. 6, between 240 and 400 °C, the thermal cleavage of the glycosidic linkage and scission of ether bonds takes place, and depolymerization to monosaccharide derivatives occurs during this stage of carbonization [60], which is illustrated in Fig. 6-product-B. These intermediates then form condensed, aromatic structures, releasing gases containing non-carbon atoms (O, H) [61]. Following heat treatment of the structure between 400 and 900 °C, the carbonaceous residue is converted into a more ordered carbon structure under inert atmosphere. Because of the complex nature of the cellulose decomposition and existence of many competing reactions involved at these stages of carbonization, the understanding of the full mechanism of aromatization resulting in graphitic products still remains a challenge.

Graphitization

The heat treatment up to 900 °C, leads to formation of semi-ordered carbonaceous structures under an inert atmosphere, and after this stage the fibres are subjected to higher temperatures to initiate graphitization. Graphitization is carried out under stress at 900–3000 °C to obtain high-modulus fibre through the development of enhanced order of the graphene stacks, both laterally between layers (crystallographic register) and in terms of preferred orientation with the fibre axis. The Young's modulus increases with the treatment temperature especially if the graphitization is conducted under tension. After graphitization the carbon content of the fibre usually increases to above 99% and the fibre density increases due to the growth of crystallites. The duration of graphitization is of the order of seconds [7].

Structure property relationship of the cellulose-based carbon fibres

The linear polymeric structure of cellulose will be subjected to drastic changes with regards to its chemistry, crystallinity and micro structure during carbonization. Although the full mechanism of carbonization of cellulose is not understood completely, a summary of some of the chemical aspects of the process is shown in Fig. 6. While a number of characterization tools are appropriate to follow this complex process [38, 60, 62–64], we will review some of the more significant ones here.

Spectroscopic techniques tend to be the most useful tools to study chemical changes on carbonization with; ^{13}C NMR Spectroscopy, Fourier transform infra-red (FTIR) spectroscopy and Raman spectroscopy being particularly appropriate.

^{13}C NMR spectra of solid carbonaceous solids usually exhibit broad lines and the distinction of different types is not easy. Chemical shift anisotropy (CSA) is the main cause of the broadening in the solid state ^{13}C NMR experiment of polycrystalline samples and can be removed by magic angle spinning (MAS). However, the averaging of the different chemical shift tensors through MAS leads to loss of some information [65]. The ^{13}C-NMR spectrum of graphite is given in Fig. 7 and is a typical example of the loss of the resolution through the MAS method. The accurate knowledge of CSA tensors is often very useful for fitting the individual peaks for detailed information. The main peaks of some carbon materials observed are given in Table 2.

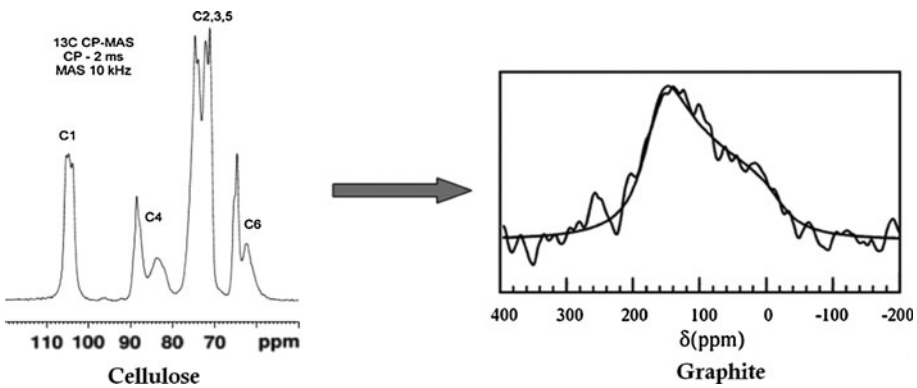

Fig. 7 Solid state ^{13}C-NMR spectrum of cellulose and graphite [65]

Table 2 Characteristic solid state ^{13}C NMR peaks of the carbonaceous materials

Carbon materials	Chemical shift (ppm)	Ref.
Diamond	35	[66]
Graphite	108–119	[67]
Polyaromatic turbostratic carbon structure	123	[68]
CNTs	124–126	[69, 70]
Carbon nanohorns	116–124	[71]

Plaisantin et al. [72] followed changes during carbonization of rayon fibres using Cross Polarized Magic Angle Spinning (CP/MAS) ^{13}C NMR, Fig. 8 and correlated the structural data with mechanical property changes. These authors interpret the development of the spectra as follows; between 300 and 500 °C, the dehydration of the glucopyranose units accompanied by ring opening, formation of ethylenic bonds and rearrangement to ketone or ester groups. From 500 to 600 °C aliphatic and phenolic carbon signals progressively disappeared while ethylenic and aromatic carbon structures appeared. At 650 °C, the ^{13}C NMR spectrum suggests that the aromatisation process is complete, as all individual carbon peaks disappear and merge as one broad peak. The mechanical properties during these stages change from elasto-plastic behaviour of cellulose, typical of an aligned polymer, to the elastic and brittle behaviour of the final carbon fibre. In the same study, the non-linear and reversible stress/strain relationship of the polymeric intermediate obtained at 500 °C is explained by a chemical structure consisting in small aromatic domains connected by oxygen linkages.

Vibrational spectroscopy such as FTIR plays a key role to study the structure of cellulose and all of the vibrational

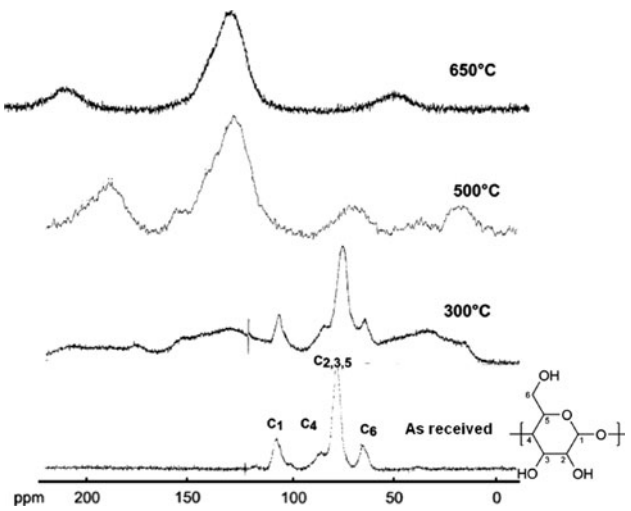

Fig. 8 ^{13}C-CP/MAS-NMR spectra of the cellulosic precursor heated at various temperatures, adapted from [72]

modes of cellulose are potentially both infrared and Raman-active. Significant information has been achieved by using FTIR method such as; the assignments for the hydroxyl frequencies [73–75] and the description of the crystalline dimorphism of native celluloses [76, 77]. Table 3 lists the intra- and intermolecular hydrogen bonds reported for native cellulose-I and -II [78].

It is also possible to follow the chemical transformations that take place when the cellulose is converted into carbonaceous products using FTIR spectroscopy. Pastorova et al. [82] studied the early stages of carbonization up to 390 °C. The analysis of the FTIR spectrum of the char produced at 200 °C was found very similar to that of cellulose. The FTIR spectra from this study clearly shows the continuous dehydration process by the decrease in the intensity of the O–H stretching band around the 3300–3400 cm^{-1} frequency range, Fig. 9a. At 1620 and 1700 cm^{-1}, two new bands begin to appear which has been assigned for the formation of C=C and C=O bonds, respectively. On the other hand, the study carried out by Low and Morterra [83] shows the structural changes on cellulose-I using IR spectra at higher temperature treatments. This study reveals that the collapse of the cellulose structure starts at 280 °C continuing through 350 °C. As the temperature is raised above 500 °C, the sp^2 type bond formation and aromatization is clearly observed, a result complementary to the ^{13}C NMR measurements.

Raman spectroscopy has some great advantages to study cellulosic samples; highly polar bond systems with relatively high dipole moments lead to very intense Raman

Table 3 IR Assignments for OH regions reported in Cellulose-I and -II

Frequency (ν-cm^{-1})	Interpretation	Ref.
3350–3340	νOH	[79, 80]
2900	νCH	[79, 80]
1636–1634	δOH (adsorbed water)	[79, 80]
1429	δsCH_2	[79, 80]
1368	δCH	[79]
1336	δOH (in plane)	[81]
1318	ωCH2 or δC–O–H	[81]
1282	δCH-bending	[81]
1200	δOH-bending	[81]
1160	ν_{as}C–O–C (anti-symmetric stretching)	[79, 81]
1105	Anti-symmetric in-phase ring stretching	[79, 81]
1061–1047	δC–O–C (pyranose ring)	[79, 81]
1036–1032	γ C–O (C6)	[82]
898	ν_{as} (ring), Anomeric vibration at β-glycosidic linkage	[79, 81]
668–665	γOH (out of plane)	[79]

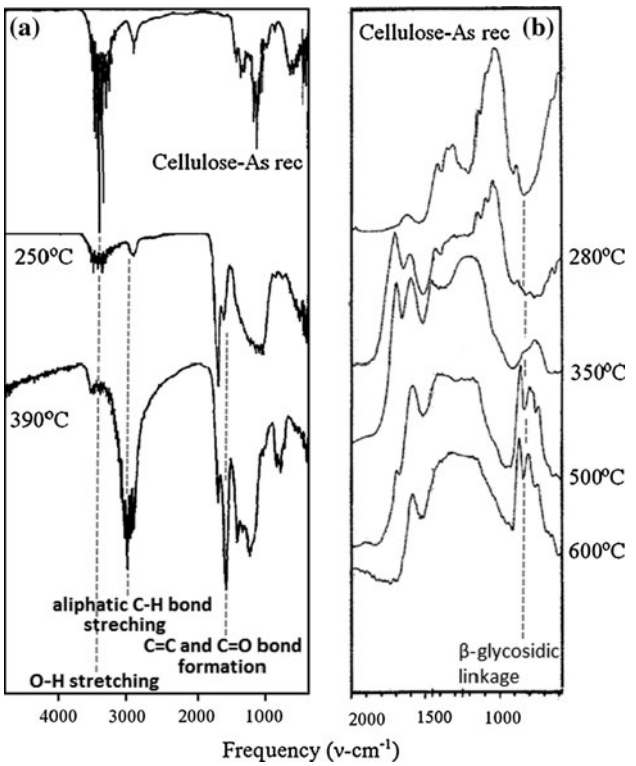

Fig. 9 FTIR spectra of cellulose taken at different segments of carbonization, adapted from [82] and [83]

bands, whereas these systems give weak IR intensities. With respect to cellulose, in the IR spectra the OH bonds and the absorbed water are the dominant features. In contrast to this, the Raman spectrum is dominated by C–C bonds in the backbone of the structure and C–H bonds. In addition, the variations in the refractive index of the cellulose lead to scattering losses which will vary with frequency over the infrared region. In Raman spectroscopy, refractive index variations are not a problem, as the excitation frequency is far removed from any absorption bands. Therefore, Raman spectra of samples such as cellulose, which scatter light strongly, are more accurate representations of the vibrational motions and the characteristic vibrational transitions [84].

Furthermore, over the past 20 years, Raman scattering has proved to be a very useful technique for investigating graphitic materials [85]. In some senses, it is complementary to X-ray (XRD) or electron microscopy techniques, which can detect lattice optical phonons and is very sensitive to planar defects associated with grapheme layer terminations which appear as a unique 'D' band in the spectra [86, 87]. Raman spectroscopy has been used to determine the stiffness of a number of materials, particularly polymeric fibres including the molecular deformation of many cellulosic materials and graphitic materials such as carbon nanofibres and carbon nanotube fibres. The technique relies on the determination of the rate of shift of a particular spectral band as a function of applied tensile or compressive deformation [88]. This shift is due to the transformation of stress in the covalent bonds along the polymer backbone and changes in the bond angles directly into macroscopic deformation [89]. The study by Hamad and Eichhorn [90] on regenerated cellulose showed that tensile stress or strain leads to a shift in the Raman band of cellulose-II structure at the 1095 cm^{-1} peak position to lower frequencies due to direct stretching of the cellulose chain.

Figure 10 in the case of carbon nanotubes, Lourie and Wagner [91], determined the Young's modulus of single- and multiwall nanotubes using a concentric cylinder model from micro-Raman spectroscopy data from compressive deformation of embedded nanotubes and Cooper et al. [92] showed that Raman spectroscopy can be used to characterise and follow the tensile deformation of SWNTs and MWNTs using 4-point bending of the dispersed material on a resin beam.

Li and Eichhorn [94] estimated the stiffness of resin embedded carbon nanowhiskers produced by pyrolysis of tunicate-based cellulose examining samples of both cellulosic precursor and pyrolysis product at 800 °C. The Raman spectra from this study are given in Fig. 11. The analysis of the shift of the G-band in the Raman spectra at 1580 cm^{-1} of the pyrolysed material came-up with a shift rate of 20.9 cm^{-1}%, which indicated a much stiffer material than the cellulosic precursor with moduli of greater than 700 GPa.

For a good carbon-fibre precursor with excellent mechanical properties, high crystallinity and a high degree of orientation along the fibre axis are required. The cellulose chain can adopt two conformations. In the cellulose I form there are two intramolecular hydrogen bonds along the same chain cellulose molecule, between O(2)–O(6) and O(3)–O(5), whereas in the cellulose-II form there is a

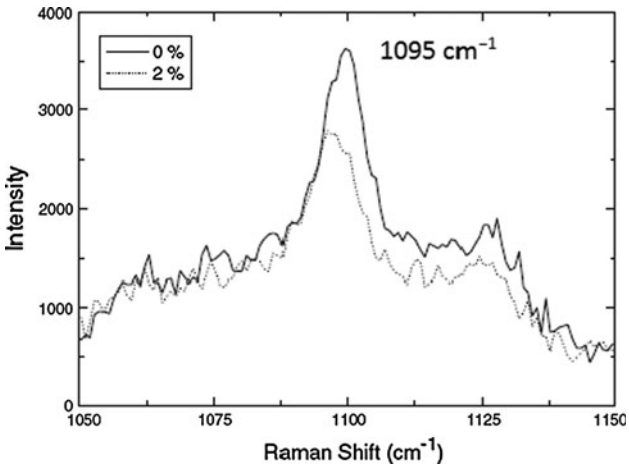

Fig. 10 Raman band at 1095 cm^{-1} relaxed and under 2% strain, adapted from [93]

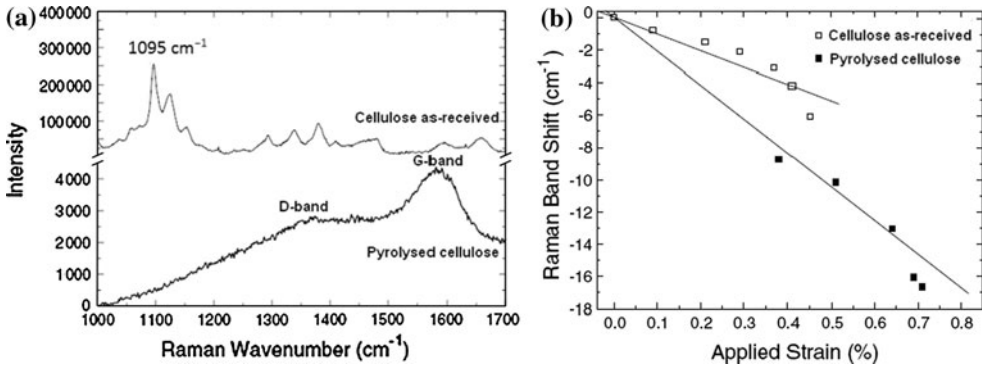

Fig. 11 **a** Raman spectra obtained from non-pyrolysed and pyrolysed cellulose samples and **b** relative Raman band shifts for the 1095 cm^{-1} C–O band from as received cellulose and 1580 cm^{-1} G-band from pyrolysed cellulose, adapted from [94]

y-branched intramolecular hydrogen bond between O(3)–O(5) and O(6) atoms as shown in Fig. 12. These two different conformations of the hydroxymethyl group cause a significant difference in the ultimate tensile properties. The modulus of the cellulose-I chain is 140 GPa whereas that of the cellulose-II chain is only 90 GPa [95, 96]. This difference explains why the dynamic tensile moduli of some native cellulose fibres are nearly 120 GPa, whereas it does not exceed 60 GPa for highly oriented regenerated cellulose fibres [97]. Therefore, the carbon-fibres produced from these two different conformations of cellulose is expected to show significant differences regarding their crystallinity and mechanical properties. Although the cellulose-I structure shows a great promise as a carbon-fibre precursor, the cellulose fibres are not being produced in cellulose-I crystalline form industrially which remains as a challenge. In terms of morphology and microstructure, the regenerated fibres (cellulose-II) can be classified as semi-crystalline and belong to the class of non-graphitizable carbons group, which is another reason why it is disadvantaged for the production of high-mechanical performance carbon fibres.

X-ray diffraction (XRD) in addition to its ability to determine the crystal structure is also valuable in the context of a study of graphitization of cellulosic fibres both in its ability to determine the paracrystallinity and crystal size through their contributions to peak width in the radial direction on a transmission X-ray pattern, as well as in its usefulness to determine the quality of the preferred orientation of the ordered (crystalline) entities in relation to the fibre axis. The latter can be determined from the azimuthal half width of equatorial reflections [99].

Previous studies on the transformation of cellulose to graphite-like crystal structure using the XRD method showed that during the thermal cleavage and depolymerization reactions between 400 and 600 °C the crystallinity of the polymer is lost [100, 101]. This generally amorphous structure with broad maxima and very little if any preferred orientation then converts to a 2D turbostratic carbon structure with grapheme layers containing the fibre axis at temperatures >900 °C. A remarkable feature is that the carbon structure formed via pyrolysis retains some memory of the starting structure through the entire process [38, 47, 100, 102]. Figure 13 shows X-ray diffraction patterns of the bacterial and ramie-based cellulose precursors, where the ramie is in the form of a fibre and the bacterial cellulose is in the unoriented film, formation of the amorphous carbon structure around 500 °C and the graphitic structure formation at 2000 °C. The graphitic arrangement shows a significant difference depending on the starting material. The unoriented bacterial cellulose showed no orientational rearrangement after the final graphitization, while in the case of highly oriented ramie fibre, the aligned fibre structure was retained when fully graphitized [100], which

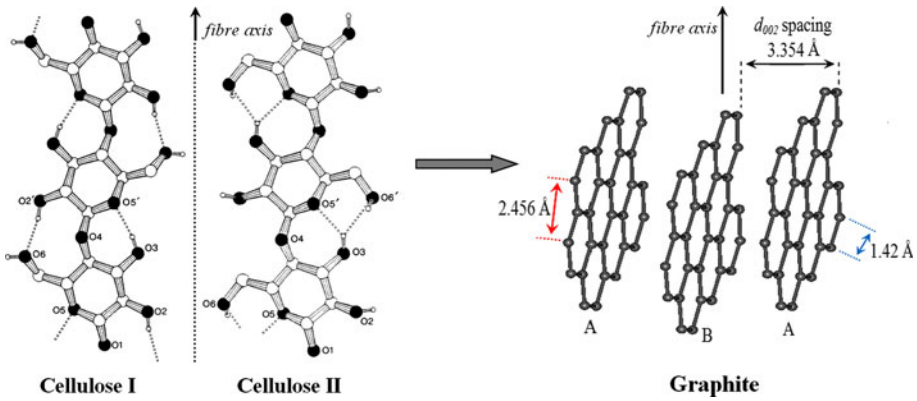

Fig. 12 Crystal structures of Cellulose-I and -II (Adapted from [98]) and Graphite

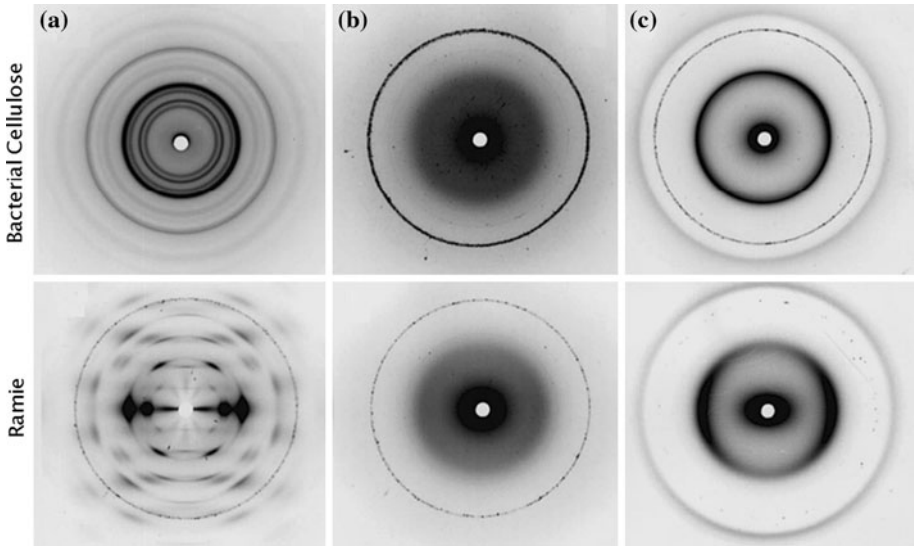

Fig. 13 X-ray patterns of **a** unoriented bacterial cellulose and ramie fibre based precursor materials, **b** amorphous carbon formation from bacterial and ramie-based cellulose at 500 °C and **c** graphitic carbon formation at 2000 °C, adapted from [100]

is in good agreement with Bacon and Tang's [47] work on the relationship between the X-ray fibre patterns of regenerated cellulose. Their study showed that oriented rayon fibre gives rise to a well oriented graphitized fibre.

In order to correlate the orientation of the graphitic layers formed to the orientation of cellulose precursor, Bacon and Tang worked on a highly oriented film of bacterial cellulose as well [47]. Figure 14 shows the relative number of cellulose (101) planes oriented at various angles ϕ away from the surface plane and profile for the graphitized film using the (002) (graphite layer) reflection The azimuthal half width of the cellulose (101) reflections is about 12° and in the case of graphite the layer planes are preferentially oriented parallel to the surface of the film, with an azimuthal half width of about 13°. This connection was interpreted by the authors [47] as a clear indication of evolution of the graphite layers from the (101) planes of the cellulose crystal.

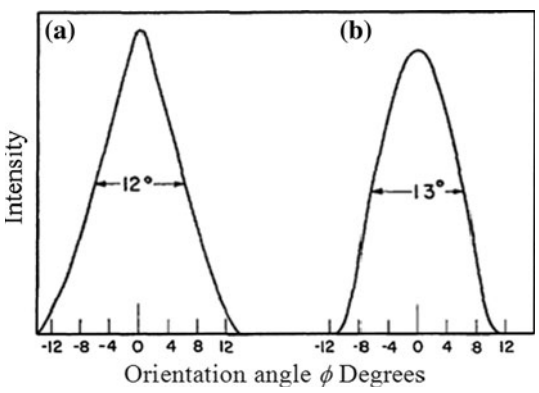

Fig. 14 Profile of X-ray scattering intensity versus orientation of crystal planes **a** (101) reflection from film of bacterial cellulose. **b** (002) reflection from graphitized bacterial cellulose [47]

The drastic changes in the chemical bonding and crystalline arrangement of cellulose will cause many changes in the microstructure as well. Cellulose forms a hierarchal microstructure, where molecular chains form individual nanofibres of cellulose. These nanofibres then form microfibres and further bundling of these microfibres forms the cellulose fibres. This hierarchal structure can easily be observed using electron microscopy as shown in Fig. 15.

In addition to good mechanical properties, as a carbon-fibre precursor, cellulose is expected to have a round cross-section and few micron-scale defects such as voids in the structure, since many of the physical features of precursor material pass on to the resulting carbon fibre through the carbonization process [103]. From the scanning electron microscope (SEM) images given in Fig. 16 it can be clearly seen that Lyocell makes a better precursor for carbon-fibre production with its round shaped cross-section, fewer defects in its cross-section and smoother surface and with its excellent alignment along the fibre axis. [30]. The study carried by Wu et al. [104] on the changes of microstructure of cellulose during carbonization using Lyocell and rayon also showed a difference between the surfaces of carbon fibres produced.

The SEM micrographs of carbon fibres from rayon and Lyocell-based precursors are given in Fig. 17. In the case of the Lyocell-based carbon fibre, being smoother than the rayon one which showed cracks and grooves. In addition, the authors found that Lyocell-based carbon fibre possessed higher strength than those of rayon-based carbon fibre, which was considered as a result of the surface and cross-sectional morphology. However, the Lyocell-based carbon fibres still showed lower mechanical properties than ideal (0.90 ± 0.1 GPa); the Scanning tunnelling microscopy (STM) analysis of the Lyocell-based carbon fibre samples from the same study showed that the hexagonal arrangement

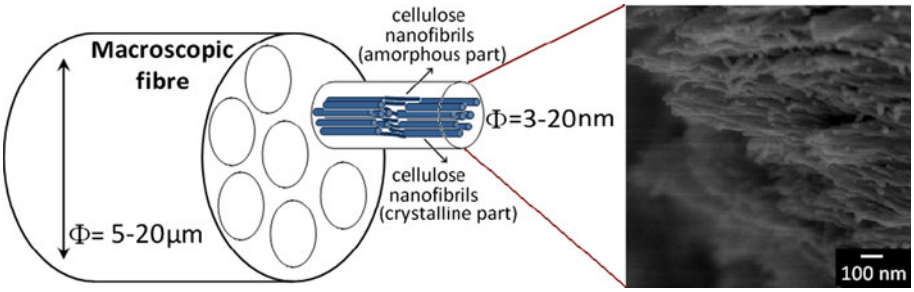

Fig. 15 The hierarchical structure of cellulose fibres and SEM Micrograph of cellulose nanofibrils

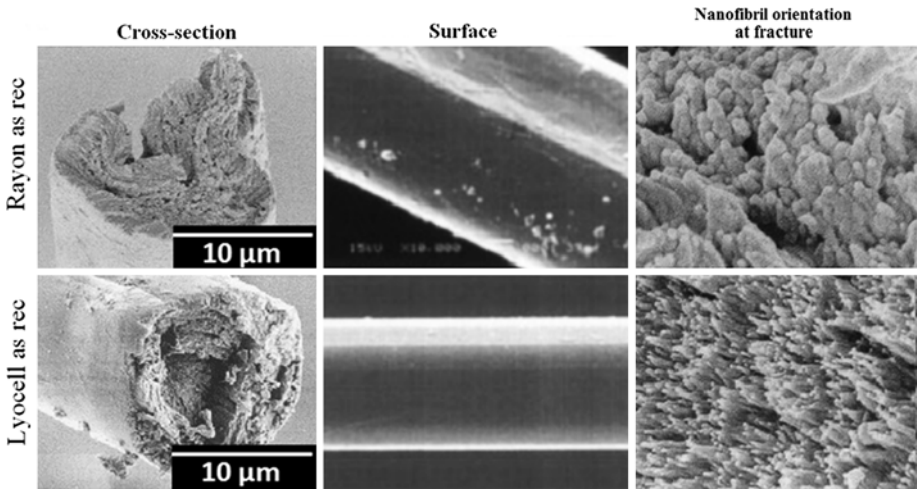

Fig. 16 SEM Micrographs of surface and cross-section morphology of cellulose fibres, adapted from [30, 105]

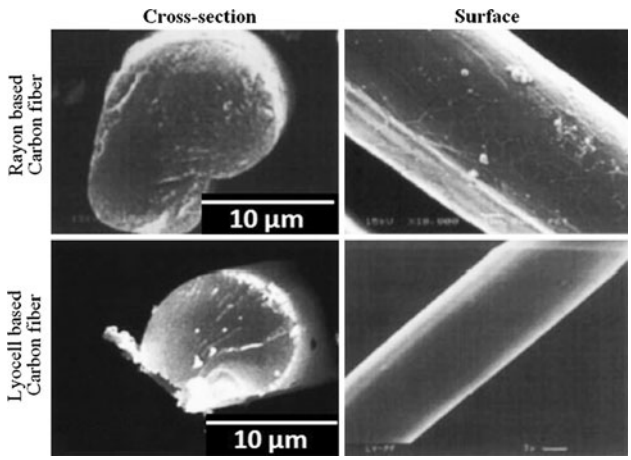

Fig. 17 SEM Micrographs of surface and cross-section morphology of cellulose-based carbon fibres

of the carbon atoms has many defects at the surface which might be the main reason for the lack of strength in cellulose-based fibres.

Cellulose fibres produced as continuous filament yarns are very suitable for carbon-fibre production. The typical fibre diameter for cellulose fibres is between 10 and 20 μm. However, it is also possible to find coarse fibres up to 60 μm thickness. Cellulose has a well-ordered crystalline structure so as long as the crystalline nanofibrils are well aligned in the fibre, one has the right basis for well-ordered and oriented graphitic structures. Therefore, the choice of a cellulose precursor with good orientation and high crystallinity is really important for cellulose-based carbon-fibre production. The crystallinity and Young's modulus of different commercially available cellulosic precursors and cellulose nanofibrils are given in Table 4. From this table Lyocell and Polynosic grades (highly oriented and high-modulus rayon fibres) stand out as good carbon fibre precursors. Again here Lyocell-based carbon fibres shows better mechanical properties, which is in good agreement with its microstructure, crystallinity and morphology as well.

Graphitic structure formation from cellulose-based fibres can also be controlled during the carbonization process by increasing the temperature and by stretching the fibres. The Young's modulus improves by increasing temperature if the graphitization is carried out under tension. The early Thornel range of carbon fibres were an example of this type. The stretching process is not as effective at the early stages of carbonization; this is partially due to the low strength of the decomposed cellulose fibres. Stretching by up to 100% under an inert atmosphere (N_2 or Ar) causes the graphitic layer planes to align better along the fibre axis direction and it is possible to produce carbon fibres with an elastic modulus ranging from 170 to 500 GPa and tensile strength from 1 to 2 GPa for some commercial fibres [106].

Table 4 Summary of the mechanical properties of cellulosic fibres

Sample	Linear density (tex[a])	Specific strength (N/tex[b])	Specific stress (N/tex[b])	Elongation at break (%)	DP	Crystallinity %	Ref.
Lyocell	0.130	0.61	7.44	6.4	550–600	70–75	[107, 108]
Viscose	0.167	0.42	3.01	16	250–350	45–48	[107, 108]
Polynosic	0.174	0.40	10.0	14	300–600		[107]
Tencel	0.130	0.40		13			[107]
Cupro	0.250	0.22	8.8	9.7	450–550		[107]
Fortisan	0.070	0.24		3.2			[107]
Celsol	0.330	0.08		7.8			[107]
CV-Tyre Cord	0.190	0.14		15			[107]
Theoretical			85–110		10,000		[109–111]
Bacterial cellulose (BC)			20–60			60–80	[112–115]
Regenerated BC fibres		0.05–0.15		3–8			[116]
Microcrystalline cellulose			12–20		140–160	60–70	[117, 118]
Flax fibres			18–30			~65	[117]
Hemp fibres			22–30			~60	[117]

[a] tex is the linear density unit which is equal to the grams per kilometre of material

[b] *N*/tex is the tensile strength unit expressed in force divided by linear density which is numerically equivalent to GPa/specific gravity

The electrical properties of various forms of carbon, including graphite, anthracite carbons, carbon nanotubes and graphene materials are of great interest in many technical areas. The electrical properties of carbon materials derived from organic precursors have been studied extensively over the years and have been shown to vary widely depending on the nature of the precursor and the heat treatment temperature (HTT) [119, 120]. It is reported that the resistivity of low modulus carbon fibres from cellulosic precursors is in the range of 30×10^{-5}–50×10^{-5} Ωm, for PAN-based CF it is 12×10^{-5}–25×10^{-5} Ωm). The resistivity decreases significantly as the fibres are graphitized; for graphitized carbon fibres from cellulosic precursors the resistivity is in the range of 3×10^{-5}–7×10^{-5} Ωm, for PAN-based CF the resistivity is 5×10^{-5}–10×10^{-5} Ωm [121] and for copper it is 1.678×10^{-8} Ω m [122].

Cellulose structure do not melt where they might be expected to show a thermotropic mesophase, nor are there any reports of molecular mesophases apparent in solution [123], unlike for substituted variants such as cellulose nitrate or hydroxypropyl [124]. Earlier studies of electronic properties of soft carbons which have shown that electrical resistivity decreases by nine orders of magnitude as temperature treatment increased from 600 to 3000 °C, resulting, in effect, in a non-metal to metal transition [125, 126].

Rhim et al. [123] studied the change in the conductivity of cellulose fibres as they were carbonized and graphitized at 1200 and 2000 °C, respectively, describing five different zones of AC and DC electrical conductivity depending on the decomposition and degree of conversion of the cellulosic materials to carbon. Cellulose has a conductivity of 10^{-8} S/cm. According to Rhim et al.; between 250 and 350 °C the electrical conductivity increases from 10^{-6} to 10^{-5} S/cm as a result of polarization of organic functional groups, however, it is then observed to decrease with further increase in treatment temperature up to 500 °C as the cellulose starts to decompose and lose the polar groups. At this stage, the material forms a system consisting of well dispersed and highly conducting nano-clusters embedded in a matrix of low conducting amorphous carbon. At 600 °C, the nano-clusters grow in size and move sufficiently close to each other to interact resulting with a non-linear frequency dependence of AC conductivity, of the order of 10^{-4} S/cm. It is over the range 610–1000 °C that the five order magnitude increase in DC conductivity (from 10^{-3} to 10^{2} S/cm) is seen. This major trend is considered to represent a combination of percolation between, as well as a rise in intrinsic conductivity of the carbon clusters. At higher temperatures up to 2000 °C, the conductivity remains comparatively constant at 10^{2} S/cm [123].

Conclusion

For the carbon fibres a constant growth in both production and consumption in the future is expected. However, most of the potential large-volume applications of carbon fibres such as automotive industry are under-developed due to the high fibre cost. Despite their comparatively poor yield on carbonization, carbon fibres produced from cellulose are competitive, and likely to become more so with on-going

increases in oil price. They are also competitive with respect to particular properties, especially thermal conductivity, high purity and mechanical flexibility, and are attracting renewed and increasing attention over the last decade. Much of the focus of current work is on the microstructure through control of precursor morphology and processing conditions. The whole area of the possible addition of low cost natural products, such as lignin to [127] cellulosic carbon fibre precursors, is also ripe for further improvement.

Acknowledgements The authors wish to thank Dr Ian Graveson of SAPPI (South African Paper and Pulp Industry) for his advice and support, Dr S. Eichhorn for helpful discussions and SAPPI for funding.

References

1. Edison TA (1892) US Patent 470925
2. Bacon R (1959) US Patent 2,957,756
3. Roger B, Cranch George E, Moyer Jr, Ralph O, Watts Willie H (1967) US Patent 3305315
4. Schalamon WA, Bacon R (1973) US Patent 3716331
5. [5] Shindo A (1961) Report from the Osaka Industrial Research Institute no. 317, Osaka
6. Morgan P (2005) Carbon fibers and their composites. CRC Press, Boca Raton
7. Huang X (2009) Materials 2:2369
8. Cohn SM, Das S (1998) A cost assessment of conventional PAN carbon fiber production technology. Energy Division, Oak Ridge National Laboratory, Tennessee
9. Graham KJ (2009) DoE advances lower-cost carbon fiber R&D, Composites Technology, 4 Apr 2009
10. Wu Q, Pan D (2002) Text Res J 72:405
11. Zhang H, Guo L, Shao H, Hu X (2006) J Appl Polym Sci 99:65
12. Watt W (1985) In: Kelly A, Rabotnov YN (eds) Handbook of composites, vol I. Elsevier Science Publishers B. V., Holland
13. Watt W (1970) Proc R Soc Lond Ser A Math Phys Sci 319:5
14. Edie DD, Fox NK, Barnett BC, Fain CC (1986) Carbon 24:477
15. Edie DD (1998) Carbon 36:345
16. Knibbs RH (1971) J Microsc Oxf 94:273
17. Bright AA, Singer LS (1979) Carbon 17:59
18. Franklin R (1951) Proc R Soc Lond A 209:196
19. Franklin R (1951) Acta Crystallogr A 4:253
20. Franklin RE (1950) J Chim Phys Physico Chim Biol 47:573
21. Ishida O, Kim DY, Kuga S, Nishiyama Y, Brown RM (2004) Cellulose 11:475
22. Minus M, Kumar S (2005) JOM J Miner Met Mater Soc 57:52
23. Bahl OP (1998) In: Donnet JB et al. (eds) Carbon fibers. Marcel Dekker, New York
24. Bacon R, Modlen GF, Frank C, McEnaney B, Blakeley TH, Manfre G (1980) Phil Trans Roy Soc Lond Math Phys Sci 294:437
25. Davidson JA, Jung HT, Hudson SD, Percec S (2000) Polymer 41:3357
26. Paiva MC, Kotasthane P, Edie DD, Ogale AA (2003) Carbon 41:1399
27. Toray Carbon Fibers America Inc (2010) http://www.toraycfa.com/product.html
28. CYTEC.COM® (2009) http://cytec.com/engineered-materials/thornel-pitch.htm
29. SOHIM,Republican Unitary Enterprise Svetlogorsk Production Association (2010) Khimvolokno. http://www.sohim.by/en/catalog/carbon/
30. Peng S, Shao H, Hu X (2003) J Appl Polym Sci 90:1941
31. Ford CE, Mitchell CV (1963) UNION CARBIDE CORP fibrous graphite. US Patent 3,107,152
32. Richard B, Millington LA, Robert C (1967) Process of graphitizing "polynosic" regenerated cellulose fibrous textile and resulting fibrous graphite textile. US Pat 3322489
33. Yoneshiga I, Teranishi H (1970) Jap. Pat. Specification 2774/70 1970
34. Zeng F, Pan D, Pan N (2005) J Inorg Org Polym Mater 15:261
35. McCorsley CC (1981) US Patent no. 4,246,221
36. Chanzy H, Paillet M, Hagege R (1990) Polymer 31:400
37. Koslow EE (2007) US Patent 7,296,691
38. Wu Q-l, Gong J-h, Zhang Z-h, Ding P (2007) New Carbon Mater 22:47
39. Tomlinson JB, Theocharis CR (1992) Carbon 30: 907
40. Kim D-Y, Nishiyama Y, Wada M, Kuga S (2001) Cellulose 8:29
41. Tang MM, Bacon R (1964) Carbon 2:211
42. Carrillo F, Defays B, Colom X, Suñol J, López-Mesas M (2009) J Therm Anal Calorim 97:945
43. Cross CB, Ecker DR, Stein OL (1964) US Patent 3,116,975
44. Brunner PH, Roberts PV (1980) Carbon 18:217
45. Abbott WF (1962) US Patent 3,053,775
46. Bacon R (1973) In: Walke JPL, Thrower P (eds) Chemistry and physics of carbon, vol 9. Marcel Dekker, New York
47. Bacon R, Tang MM (1964) Carbon 2: 221, IN3–IN4, 3–5
48. Plaisantin H, Pailler R, Guette A, Birot M, Pillot JP, Daude G, Olry P (2006) J Mater Sci 41:1959. doi:10.1007/s10853-006-1297-8
49. Sevilla M, Fuertes AB (2009) Carbon 47:2281
50. Shunjin P, Huili S, Xuechao H (2003) J Appl Polym Sci 90:1941
51. Domvoglou D, Wortmann F, Taylor J, Ibbett R (2010) Cellulose 17: 757
52. Gentry SJ, Howarth SR (1984) Sensors Actuators 5:265
53. Kilzer FJ, Broido A (1965) Pyrodynamics 2:151
54. Piskorz J, Radlein DSAG, Scott DS, Czernik S (1989) J Anal Appl Pyrol 16:127
55. Trushnikov AM, Kazakov ME, Gridina YM, Vazheva LD, Borisova LK (1995) Russian Patent 2047674
56. Kazakov ME, Trushnikov AM, Yunitskaia ML (1995) Russian Patent 2045472
57. Lysenko AA, Piskunova IA, Astashkina OV (2003) Fibre Chem 35:189
58. Kaverov AT, Kazakov ME, Varshavsky VY (1995) In: Kostikov VI (ed) Fibre science and technology. Chapman & Hall, London
59. Aksel S, Eder D (2010) J Mater Chem 20: 9149
60. Kawamoto H, Murayama M, Saka S (2003) J Wood Sci 49:469
61. Lie JA, Hägg M-B (2006) J Membr Sci 284:79
62. Wu Q, Pan N, Deng K, Pan D (2008) Carbohydr Polym 72:222
63. Ali M, Apperley D, Eley C, Emsley A, Harris R (1996) Cellulose 3:77
64. Wu Q-l, Gong J-h, Zhang Z-h, Pan D (2007) Carbon 45:1378
65. Darmstadt H, Roy C, Kaliaguine S, Xu G, Auger M, Tuel A, Ramaswamy V (2000) Carbon 38:1279
66. McNamara KM, Gleason KK (1992) J Appl Phys 71:2884
67. Goze-Bac C, Latil S, Lauginie P, Jourdain V, Conard J, Duclaux L, Rubio A, Bernier P (2002) Carbon 40:1825
68. Dobrovol'skaya IP, Mokeev MV, Sazanov YN, Gribanov AV, Sukhanova TE (2006) Russ J Appl Chem 79:1312
69. Tang X-P, Kleinhammes A, Shimoda H, Fleming L, Bennoune KY, Sinha S, Bower C, Zhou O, Wu Y (2000) Science 288:492
70. Goze-Bac C, Latil S, Vaccarini L, Bernier P, Gaveau P, Tahir S (2001) Phys Rev B 63:100302
71. Imai H, Babu PK, Oldfield E, Wieckowski A, Kasuya D, Azami T, Shimakawa Y, Yudasaka M, Kubo Y, Iijima S (2006) Phys Rev B 73:125405
72. Plaisantin H, Pailler R, Guette A, Daudé G, Pétraud M, Barbe B, Birot M, Pillot JP, Olry P (2001) Compos Sci Technol 61:2063

73. Marrinan HJ, Mann J (1956) J Polym Sci 21:301
74. Tsuboi M (1957) J Polym Sci 25:159
75. Liang CY, Marchessault RH (1959) J Polym Sci 37:385
76. Atalla RH, Vanderhart DL (1984) Science 223:283
77. VanderHart DL, Atalla RH (1984) Macromolecules 17:1465
78. Kondo T (1997) Cellulose 4:281
79. Kondo T, Sawatari C (1996) Polymer 37:393
80. Fengel D, Strobel C (1994) Acta Polym 45:319
81. Hulleman SHD, van Hazendonk JM, van Dam JEG (1994) Carbohydr Res 261:163
82. Pastorova I, Botto RE, Arisz PW, Boon JJ (1994) Carbohydr Res 262:27
83. Low MJD, Morterra C (1985) Carbon 23:311
84. Wiley JH, Atalia RH (1987) Carbohydr Res 160:113
85. Dresselhaus MS, Eklund PC (2000) Adv Phys 49:705
86. Dresselhaus MS, Dresselhaus G, Sugihara K, Spain IL, Goldberg HA (1988) In: Graphite fibers and filaments. Springer, Berlin
87. Endo M, Kim VA, Nishimura K, Hayashi T, Matushita T (2001) In: Rand B, Appleyard SP, Yardim MF (eds) Nato series, 374, Academic Publishers, Amsterdam
88. Young RJ (1995) J Text Inst 86:360
89. Treloar LRG (1960) Polymer 1:95
90. Hamad WY, Eichhorn S (1997) J Eng Mater Technol 119:309
91. Lourie O, Wagner HD (1998) J Mater Res 13:2418
92. Cooper CA, Young RJ, Halsall M (2001) Compos Part A Appl Sci Manuf 32: 401
93. Hsieh Y-C, Yano H, Nogi M, Eichhorn SJ (2008) Cellulose 15:507
94. Li N, Eichhorn S (2006) J Mater Sci 41:4993. doi:10.1007/s10853-006-0138-0
95. Kroon-Batenburg LMJ, Kroon J, Northolt MG (1986) Polym Commun Guildford 27:290
96. Northolt MG, De Vries H (1985) Die Angew Makromol Chem 133:183
97. Northolt MG, van der Hout R (1985) Polymer 26:310
98. Northolt MG, Boerstoel H, Maatman H, Huisman R, Veurink J, Elzerman H (2001) Polymer 42:8249
99. Chari SS, Bahl OP, Mathur RB (1981) Fibre Sci Technol 15:153
100. Kim D-Y, Nishiyama Y, Wada M, Kuga S (2001) Carbon 39:1051
101. Sevilla M, Fuertes AB (2010) Chem Phys Lett 490: 63
102. Ruland W (1969) J Polym Sci Part C Polym Symp 28:143
103. Peng S, Shao H, Hu X (2004) Int J Polym Mater 53:601
104. Wu Q-L, Gu S-Y, Gong J-H, Pan D (2006) Synth Metals 156:792
105. Fink HP, Weigel P, Purz HJ, Ganster J (2001) Prog Polym Sci 26:1473
106. Venner JG (2000) In: Kirk-Othmer encyclopaedia of chemical technology, Wiley Inc., New York
107. Röder T, Moosbauer J, Kliba G, Schlader S, Zuckerstätter G (2009) Lenzinger Berichte 87:98
108. Sfiligoj Smole M, Persin Z, Kreze T, Stana Kleinschek K, Ribitsch V, Neumayer S (2003) Mater Res Innov 7:275
109. Marhöfer RJ, Reiling S, Brickmann J (1996) Ber Bunsenges Physikalishe Chem 100:1350
110. Sakurada I, Nukushina Y, Ito T (1962) J Polym Sci 57:651
111. Tashiro K, Kobayashi M (1985) Polym Bull (Berlin) 14:213
112. Guhados G, Wan W, Hutter JL (2005) Langmuir 21:6642
113. Watanabe K, Tabuchi M, Morinaga Y, Yoshinaga F (1998) Cellulose 5:187
114. Yamanaka S (1989) J Mater Sci 24:3141. doi:10.1007/BF01139032
115. Nishi Y, Uryu M, Yamanaka S, Watanabe K, Kitamura N, Iguchi M, Mitsuhashi S (1990) J Mater Sci 25:2997. doi:10.1007/BF00584917
116. Gao Q, Shen X, Lu X (2011) Carbohydr Polym 83: 1253
117. Eichhorn S, Young RJ (2001) Cellulose 8:197
118. Ardizzone S, Dioguardi FS, Mussini T, Mussini PR, Rondinini S, Vercelli B, Vertova A (1999) Cellulose 6:57
119. Kennedy LJ, Vijaya JJ, Sekaran G (2005) Mater Chem Phys 91:471
120. Fung AWP, Dresselhaus MS, Endo M (1993) Phys Rev B 48:14953
121. Perepelkin KE (2002) Fibre Chem 34:271
122. Lide DR (1994) In: CRC handbook of chemistry and physics, 75th edn. CRC Press, Boca Raton, p 12
123. Rhim Y-R, Zhang D, Fairbrother DH, Wepasnick KA, Livi KJ, Bodnar RJ, Nagle DC (2010) Carbon 48: 1012
124. Werbowyj RS, Gray DG (1976) Mol Crystals Liquid Cryst 34:97
125. Loebner EE (1956) Phys Rev 102:46
126. Carmona F, Delhaes P, Keryer G, Manceau JP (1974) Solid State Commun 14:1183
127. Kadla JF, Kubo S, Venditti RA, Gilbert RD, Compere AL, Griffith W (2002) Carbon 40:2913